Photoaffinity Labeling with 8-Azidoadenosine and Its Derivatives: Chemistry of Closed and Opened Adenosine Diazaquinodimethanes†

Dmitrii Polshakov,‡ Saroj Rai,‡ R. Marshall Wilson,*,§ Eric T. Mack,§ Martin Vogel,§ Jeanette A. Krause,§ Gotard Burdzinski,‡,|| and Matthew S. Platz*,‡

Department of Chemistry, The Ohio State University, Columbus, Ohio 43210, Department of Chemistry, University of Cincinnati, Cincinnati, Ohio 45221, and Quantum Electronics Laboratory, Adam Mickiewicz University, Poznan, Poland 61-614

Received May 10, 2005; Revised Manuscript Received June 12, 2005

ABSTRACT: The reactive intermediate produced upon photolysis of 8-azidoadenosine was studied by chemical trapping studies, laser flash photolysis with UV−vis and IR detection, and modern computational chemistry. It is concluded that photolysis of 8-azidoadenosine in aqueous solution releases the corresponding singlet nitrene which rapidly tautomerizes to form a closed adenosine diazaquinodimethane in less than 400 fs. A perbenzoylated derivative of 8-azidoadenosine cannot undergo this tautomerization, and instead, it fragments upon photolysis to form an opened adenosine diazaquinodimethane. The singlet nitrene is too short-lived to be observed and, thus, to relax to the lowest triplet state or to become covalently attached to targeted biological macromolecules. The pivotal closed adenosine diazaquinodimethane, the product of nitrene tautomerization, has a lifetime of ca. 1 min or longer in water and in HEPES buffer at ambient temperature. However, this intermediate reacts rapidly with good nucleophiles such as amines, thiols, and phenolates, and significantly more slowly with weak nucleophiles such as alcohols and water. On the basis of these studies, it is clear that the closed adenosine diazaquinodimethane, and not the singlet or triplet nitrene, is the pivotal reactive intermediate involved in photolabeling and cross-linking studies using the 8-azidoadenosine family of photoaffinity labeling reagents.

Haley first investigated the possibility that 8-azidoadenosine, **1a**, might serve as a photoaffinity label ∼20 years ago (*1*). A family of reagents based upon **1a** has since become widely used in photoaffinity labeling and in cross-linking studies (*2*). Since adenosine is an integral part of many of the most important cofactors, ATP, NAD, FAD, CoA, and *S*-adenosylmethionine, this technology has been primarily developed for the study of adenosine cofactors and their interactions in numerous enzyme systems. However, the same technology offers great promise in defining interactions in many RNA−RNA and RNA−protein systems as well. As a foundation in the design of experiments of this type, it is most important to understand the processes by which intermediates derived from **1a** bind to and react with targeted proteins and nucleic acids, and the limitations of these processes. It has been assumed (*3*) that the photochemistry of **1a** will resemble that of aryl azides and produce short-lived nitrenes (*4*, *5*) that will indiscriminately react with residues of the macromolecular target present in the binding site (Figure 1).

In this work, we have investigated the photochemistry of 8-azidoadenosine (**1a**), 8-azido-N^9-benzyladenine (**1b**), 8-azido-N^9-methyladenine (**1c**), and 8-azidoadenine (**1d**), as well as the pentabenzoylated derivative of 8-azidoadenosine **2**. On the basis of these studies, reported below, it is evident that the pivotal intermediate in this type of photoaffinity labeling is not the nitrene itself, but closed and opened adenosine diazaquinodimethanes instead, presumably derived from the singlet nitrene.

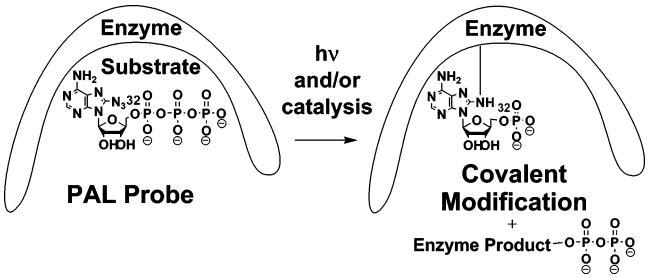

FIGURE 1: General photoaffinity labeling strategy assuming that the reactive intermediate responsible for labeling is a nitrene species.

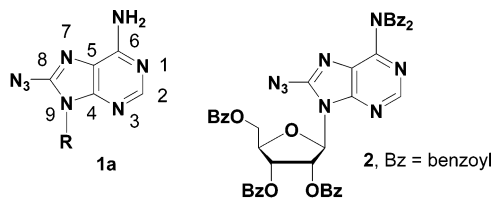

Throughout this paper:
No letter = generic
a = ribose
b = -CH_2Ph
c = -CH_3
d = -H

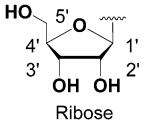

† This work was supported by NSF Grant MRI-CHE-0215950 and The Ohio Super Computer Center.

* To whom correspondence should be addressed. Phone: (614) 292-0401. Fax: (614) 292-5151. E-mail: platz@chemistry.ohio-state.edu.
‡ The Ohio State University.
§ University of Cincinnati.
|| Adam Mickiewicz University.

10.1021/bi050859z CCC: $30.25
Published on Web 07/29/2005

MATERIALS AND METHODS

General Supporting Information

Unless stated otherwise, all reactions were carried out under argon. All chemicals were purchased from Aldrich and Acros Organics. Preparative irradiations were conducted using an argon ion laser with the appropriate wavelengths provided in the text. Removal of solvents under reduced pressure was performed with a Büchi rotary evaporator connected to a water aspirator. Trace solvents were removed from products using a high-vacuum pump. Analytical TLC was conducted using E. Merck plastic-backed sheets of silica gel 60 F254. Column chromatography was performed using E. Merck silica gel 230−400 mesh size. Infrared spectrometry was carried out using a Perkin-Elmer 1600 Series FT-IR or a Perkin-Elmer Spectrum v3.02 FT-IR spectrometer. Infrared spectra were recorded in KBr pellets. Ultraviolet−visible (UV−vis) absorption spectra were obtained with a Hewlett-Packard 8453 UV−visible spectrometer. ^{1}H NMR spectra were obtained with a Bruker Avance 400 instrument. All chemical shifts are reported in parts per million downfield (δ) from TMS, using the residual DMSO as an internal standard. Abbreviations s, d, t, q, qt, and m refer to singlet, doublet, triplet, quartet, quintet, and multiplet, respectively. Coupling constants (J) are reported in hertz. In the NMR characterization of the following compounds, we have assigned a resonance to a particular carbon or proton using the numbering system shown above. These signals have been assigned through a combination of ^{1}H NMR, ^{13}C NMR, ^{1}H−^{1}H COSY, NOESY, HSQC, and HMBC experiments. High-resolution mass spectra (HRMS) were obtained using a Micromass QTOF 2 instrument.

Nanosecond Time-Resolved Laser Flash Photolysis (LFP)

A Nd:YAG laser (Spectra Physics LAB-150-10, 266 nm, 5 ns, 50 mJ) or XeCl excimer laser (Lambda Physik, 20 ns, 50 mJ, 308 nm) was used as the excitation light source. The spectrometer has been described previously (*6*). Typically, solutions were prepared in dry spectroscopic grade solvents to an optical density (OD) of ∼1.5−2.0 at the excitation wavelength (266 or 308 nm). Doubly distilled water was used to prepare water and buffer solutions. In these experiments, the samples were contained in a quartz cuvette placed in a quartz cryostat at ambient temperature. The sample solutions were changed after every laser shot, unless otherwise indicated.

Ultrafast Spectroscopy

A Ti:sapphire laser/amplifier system consists of a short pulse oscillator (Coherent/Positive Light, Mira) generating ∼40 fs pulses at ∼800 nm that seeds a regenerative amplifier (Coherent/Positive Light, Legend HE USP). The amplifier provides a 1 kHz train of ∼50 fs pulses, centered around 800 nm, with 2.7 mJ of energy/pulse. A portion of the output of the amplifier (0.9 mJ) is used to pump the optical parametric amplifier (Coherent, OPerA) equipped with the sum frequency mixing module (Coherent, SFG) to generate pump 270 nm pulses. Typical probe pulse energies were 3−5 μJ at the sample location. The pump beam is chopped with a frequency of 500 Hz. Probe pulses between 370 and 750 nm were generated by focusing a portion of the laser fundamental (<1%) into a 1 cm water cell. The probe beam is passed through an optical delay line consisting of a retroreflector mounted on a computer-controlled motorized translation stage. This is followed by interference filtering. Transmission signals were detected by Si photodiodes and measured with a digital lock-in amplifier (SRS 830). The samples were circulated in a flow cell with optical path length of 2 mm. Polarization of the pump and probe was set to the magic angle (54.7°). The instrument response was approximately 400 fs [Gaussian full width at half-maximum (fwhm)], which was determined by difference frequency mixing between the 270 nm pump beam and the 10 nm portion of the continuum in a thin BBO crystal.

Time-Resolved Infrared (TRIR) Studies

The TRIR apparatus (JASCO TRIR-1000) and technique have been described elsewhere (*7*). Briefly, a reservoir of deoxygenated sample solution (10 mL of 5 mM **1a** or **2**) was continuously circulated in a cell between two barium fluoride salt plates with a 0.5 mm path. The cell was connected to a peristaltic pump by Teflon tubes. The sample was excited by 266 nm laser pulses from a Nd:YAG laser (50 Hz repetition rate, 0.6−0.9 mJ/pulse), which is crossed with the broadband output of a $MoSi_2$ IR source (JASCO). The detection system includes a MCT photovoltaic IR detector (Kolmar Technologies, KMPV11-1-J1), with a 50 ns rise time, amplified with a low-noise differential amplifier (NF Electronic Instruments 5307), and digitized with a Tektronix TDS784D oscilloscope.

Computational Chemistry

The geometries of the singlet and triplet states of **2c** were fully optimized at the CASSCF/6-31G* (5D) level (*8*, *9*). Dynamic electron correlation was included using CASPT2/6-31G* (5D) calculations (*10*) with the CASSCF optimized geometries. Both CASSCF and CASPT2 calculations were carried out with MOLCAS (version 5.0) (*11*).

To compute the possible reaction pathways of the singlet nitrene, geometries of proposed reactive intermediates and transition states were fully optimized using the B3LYP (*12*) method with the 6-31G* (6D) basis set. Vibrational frequencies were calculated to analyze the nature of the stationary points (minimum or transition state) and were used to account for ZPE differences. For the transition states connecting the closed-shell singlet nitrene and a closed-shell intermediate, standard DFT[1] calculations were used. The solvent effect was modeled using the PCM method (*13*). All charge density data were obtained by a natural population analysis at the MP2/6-31G* level (*14*). Time-dependent DFT (TD-DFT) calculations (*15*) were performed at the B3LYP/6-31+G** level. All DFT calculations were carried out with GAUSSIAN 98 (*16*) at the Ohio Super Computer Center.

Preparation of Adenosine and Adenine Compounds

*Preparation of 8-Azidoadenosine (**1a**) and 8-Amino-N^6,N^6,$O^{2'}$,$O^{3'}$,$O^{5'}$-pentabenzoyladenosine (**2**).* Azidoadenosine **1a** was prepared from adenosine via bromination and reaction

[1] Abbreviations: DFT, density functional theory; TD-DFT, time-dependent density functional theory; 2MTHF, 2-methyltetrahydrofuran; NBS, *N*-bromosuccinimide.

with sodium azide (*17*, *18*). Its pentabenzoylated analogue **2** was prepared by the benzoylation of adenosine with benzoyl chloride followed by bromination and reaction with sodium azide (*19*). Both materials, **1a** and **2**, had spectroscopic properties consistent with those reported in the literature.

*Preparation of 8-Aminoadenosine (**3a**).* The 8-amino derivative of adenosine **3a** was prepared by a modification of the procedure of Holmes and Robins (*18*), and its detailed NMR spectroscopic properties are reported here, since they provide important standards for compounds subsequently described. A stirred solution of 8-azidoadenosine (**1a**) (0.5 g, 0.162 mmol) and rhodium on carbon (0.20 g), at 23 °C, in H_2O (50 mL), was placed under H_2 (>1 atm). After 5 h, the catalyst was removed by filtration and the solvent removed to yield **3a** as a white solid (0.450 g, 0.159 mmol, 98% yield): $C_{10}H_{14}N_6O_4$; molecular weight 282.26 g/mol; mp 165−167 °C. UV−vis and ^{1}H NMR consistent with ref *18*: UV−vis (λ_{max}, H_2O) 274 nm, reported 273 nm (16 400 M^{-1} cm^{-1}); ^{1}H NMR (DMSO-d_6, 400 MHz) δ 7.91 (s, 1H), 6.66 (s, 2H, exchangeable with D_2O), 6.60 (s, 2H, exchangeable with D_2O), 5.88 (s, 1H, exchangeable with D_2O), 5.87 (d, J = 7.2 Hz, 1H), 5.30 (d, J = 6.5, 1H, exchangeable with D_2O), 5.22 (s, 1H, exchangeable with D_2O), 4.71 (dd, J = 6.0 Hz, 1H), 4.14 (m, 1H), 3.98 (m, 1H), 3.63 (m, 2H); ^{13}C NMR (DMSO-d_6, 100.6 MHz) δ 152.8 (C_6), 152.1 (C_8), 149.7 (C_4), 148.8 (C_2), 117.5 (C_5), 87.1 (C_1'), 86.2 (C_4'), 71.4 (C_2' or C_3'), 71.3 (C_2' or C_3'), 62.2 (C_5').

Irradiation and Product Characterization

*Irradiation of 8-Azidoadenosine (**1a**) in Methanol.* A solution of 8-azidoadenosine (**1a**) (0.308 g, 1.0 mmol) at 23 °C, in dry MeOH (8 mL), was irradiated for 2 h with all the UV lines (1.38 W) of an argon ion laser open to the atmosphere. The solvent was removed under reduced pressure to yield a red oil. The red oil was purified by flash chromatography (24 g of silica gel, 20% CH_3OH in $CHCl_3$) to afford the following products.

*Isolation of 8-Aminoadenosine (**3a**).* The 8-amino compound **3a** was isolated as a white solid (0.056 g, 0.198 mmol, 20% yield): $C_{10}H_{14}N_6O_4$; molecular weight 282.26 g/mol; mp 165−167 °C. The spectral data were consistent with an authentic sample prepared as described above (*18*) and previously observed by Bose (*20*).

*Isolation of 8-Amino-2-methoxyadenosine (**4a**).* The methanol adduct **4a** was obtained as a colorless solid (0.014 g, 0.045 mmol, 5% yield): $C_{11}H_{16}N_6O_5$; molecular weight 312.12 g/mol; mp not available; R_f = 0.26 (30% CH_3OH in $CHCl_3$); ^{1}H NMR (DMSO-d_6, 400 MHz) δ 6.55 (s, 2H, exchangeable with D_2O), 6.34 (s, 2H, exchangeable with D_2O), 5.87 (d, J = 7.2 Hz, 1H), 5.56 (t, J = 5.6 Hz, 1H, exchangeable with D_2O), 5.24 (d, J = 6.4 Hz, 1H, exchangeable with D_2O), 5.15 (d, J = 4.4 Hz, 1H, exchangeable with D_2O), 4.70 (dd, J = 6.0 Hz, 1H), 4.13 (m, 1H), 3.91 (m, 1H), 3.75 (s, 3H), 3.60 (m, 2H); ^{13}C NMR (DMSO-d_6, 100.6 MHz) δ 159.6 (C_2), 153.6 (C_6), 151.4 (C_4 or C_8), 151.1 (C_4 or C_8), 112.8 (C_5), 87.0 (C_1'), 85.8 (C_4'), 71.2 (C_2' or C_3'), 71.1 (C_2' or C_3'), 62.1 (C_5') 54.2 (OCH_3); IR (KBr) ν_{max} 3352 (s and br), 2926 (w), 1628 (s), 1606 (s), 1472 (m), 1242 (m), 1077 (m) cm^{-1}; HRMS (ESI, Q-TOFMS) *m/z* calcd for $C_{11}H_{17}N_6O_5$ 313.1260, found 313.1272; UV−vis (λ_{max}, H_2O), 257, 283 nm.

*Isolation of 8-Amino-2-methoxy-6-formamidoadenosine (**5a**).* The formamide of 8-amino-2-methoxyadenosine, **5a**, was obtained as a colorless solid (0.024 g, 0.071 mmol, 7% yield): $C_{12}H_{16}N_6O_6$; molecular weight 340.29 g/mol; mp >150 °C dec; R_f = 0.36 (30% CH_3OH in $CHCl_3$); ^{1}H NMR (DMSO-d_6, 400 MHz) δ 10.63 (d, J = 10.0 Hz, 1H, exchangeable with D_2O), 9.33 (d, J = 10.0 Hz, 1H), 6.83 (s, 2H, exchangeable with D_2O), 5.89 (d, J = 7.2 Hz, 1H), 5.51 (t, J = 4.8 Hz, 1H, exchangeable with D_2O), 5.32 (d, J = 6.4 Hz, 1H, exchangeable with D_2O), 5.13 (d, J = 4.0 Hz, 1H, exchangeable with D_2O), 4.63 (dd, J = 12.4 Hz, J = 6.4 Hz, 1H), 4.12 (m, 1H), 3.98 (s, 3H), 3.93 (m, 1H), 3.62 (m, 2H); ^{13}C NMR (DMSO-d_6, 100.6 MHz) δ 163.8 (formamide), 156.8 (C_2), 154.1 (C_4), 152.9 (C_8), 149.1 (C_6), 116.2 (C_5), 86.8 (C_1'), 85.9 (C_4'), 71.2 (C_3'), 70.7 (C_2'), 61.8 (C_5'), 54.1 (OCH_3); IR (KBr) ν_{max} 3356 (s and br), 2929 (w), 1647 (s), 1603 (s), 1475 (m), 1369 (m), 1076 (m) cm^{-1}; HRMS (ESI, Q-TOFMS) *m/z* calcd for $C_{12}H_{17}N_6O_6$ 341.1210, found 341.1212; UV−vis (λ_{max}, H_2O) 284 nm (12 500 M^{-1} cm^{-1}).

*Isolation of 8-Amino-O^6-methylguanosine (**6a**).* The isomeric methanol adduct **6a** was obtained as a colorless solid (0.021 g, 0.067 mmol, 7% yield): $C_{11}H_{16}N_6O_5$; molecular weight 312.12 g/mol; mp >140 °C dec; R_f = 0.34 (30% CH_3OH in $CHCl_3$); ^{1}H NMR (DMSO-d_6, 400 MHz) δ 6.34 (s, 2H, exchangeable with D_2O), 5.91 (s, 2H, exchangeable with D_2O), 5.83 (d, J = 7.6 Hz, 1H), 5.61 (t, J = 5.2 Hz, 1H, exchangeable with D_2O), 5.24 (d, J = 6.4 Hz, 1H, exchangeable with D_2O), 5.05 (d, J = 4.0 Hz, 1H, exchangeable with D_2O), 4.58 (dd, J = 6.4 Hz, 1H), 4.09 (m, 1H), 3.90 (m, 1H), 3.88 (s, 3H), 3.62 (m, 2H); ^{13}C NMR (DMSO-d_6, 100.6 MHz) δ 157.5 (C_2), 157.5 (C_6), 155.0 (C_4), 151. (C_8), 111.5 (C_5), 86.5 (C_1'), 85.7 (C_4'), 71.3 (C_3'), 70.7 (C_2'), 61.9 (C_5') 53.4 (OCH_3); IR (KBr) ν_{max} 3360 (s and br), 2934 (w), 1630 (s), 1606 (s), 1472 (m), 1242 (m), 1076 (m) cm^{-1}; HRMS (ESI, Q-TOFMS) *m/z* calcd for $C_{11}H_{17}N_6O_5$ 313.1260, found 313.1275; UV−vis (λ_{max}, H_2O), 256 (12 580 M^{-1} cm^{-1}), 293 nm (10 090 M^{-1} cm^{-1}).

*X-ray Crystallographic Structure Determination of 8-Amino-O^6-methylguanosine (**6a**).* Crystals were obtained as colorless blocks from CH_3OH. For X-ray examination and data collection, a suitable crystal, with approximate dimensions of 0.19 mm × 0.15 mm × 0.15 mm, was mounted in a Cryo loop with paratone-N and transferred immediately to the goniostat bathed in a cold stream.

Intensity data were collected at 150 K on a standard Bruker SMART6000 CCD diffractometer using graphite-monochromated Cu Kα radiation (λ = 1.54178 Å). The detector was set 5.165 cm from the crystal. A series of 10 s data frames measured at 0.3° increments of ω were collected to calculate a unit cell. For data collection, frames were measured for a duration of 10 s at 0.3° intervals of ω with a maximum θ value of ~135°. The data frames were processed using SAINT. The data were corrected for decay, Lorentz, and polarization effects as well as absorption and beam corrections based on the multiscan technique.

The structure was determined by a combination of direct methods SHELXTL version 6.14 and the difference Fourier technique and refined by full-matrix least squares on F_2. Nonhydrogen atoms were refined with anisotropic displacement parameters. Weights were assigned as follows: $w - 1 = [\sigma^2(F_o^2) + (0.1612P)^2 + 5.1309P]$, where $P = 0.33333F_o^2$

+ 0.66667F_c^2. H atoms were either located directly or calculated on the basis of geometric criteria and were treated with a riding model. The isotropic displacement parameters for the H atoms of the cation were defined as the aU_{eq} of the adjacent atom (a = 1.5 for −OH and $-CH_3$; a = 1.2 for all others). The methanol solvent of crystallization is disordered. The model for two reasonable alternate oxygen atom (O1S and O2S) positions is presented with the conformers in an 85/15 ratio. The disorder for the carbon atom (C1S) was not addressed, and the methyl H atoms for the minor conformer are not included. Partial occupancy waters are also present in the lattice. The best fit model is presented; however, large thermal motion is associated with some of the oxygen atoms which is indicative of unresolved disorder. There may well be other partial water molecules in the lattice; some voids are present in the lattice where diffuse, disordered water may potentially reside. The refinement converged with the following crystallographic agreement factors: R1 = 6.89% and wR2 = 19.79% for 5762 reflections where $I > 2\sigma(I)$ (R1 = 6.99% and wR2 = 20.00% for all data) and 471 variable parameters (*21*).

*Irradiation of 8-Azido-N⁶,N⁶,O²′,O³′,O⁵′-pentabenzoyladenosine (**2**) in Methanol.* A solution of 8-azido-N^6,N^6,$O^{2'}$,$O^{3'}$,-$O^{5'}$-pentabenzoyladenosine (**2**) (0.020 g, 0.024 mmol) and ammonium tetrafluoroborate (0.0029 g, 0.028 mmol) in CH_3-OH (20 mL) and benzene (2 mL) was degassed and irradiated for 60 min in a Rayonet photoreactor with 350 nm lamps. The solvent was removed under reduced pressure and the residue purified by HPLC.

*Isolation of 8-Amino-N⁶,N⁶,O²′,O³′,O⁵′-pentabenzoyladenosine (**7**).* The amine **7** was obtained as a colorless solid (1.2−1.5 mg, 0.0014−0.0019 mmol, 6−8% yield): $C_{45}H_{34}N_6O_9$; molecular weight 802.79 g/mol; mp 119−121 °C; ^{1}H NMR ($CDCl_3$, 250 MHz) δ 8.36 (s, 1H), 8.04 (d, J = 7.3 Hz, 2H), 7.97 (d, J = 8.1 Hz, 2H), 7.91 (d, J = 7.3 Hz, 2H), 7.81 (d, J = 7.7 Hz, 4H), 7.56 (t, J = 7.3 Hz, 3H), 7.29−7.44 (complex, 12H), 6.23 (dd, J = 5.1 Hz, J = 5.1 Hz, 1H), 6.18 (d, J = 5.5 Hz, 1H), 6.08 (dd, J = 5.4 Hz, J = 5.4 Hz, 1H), 5.97 (bs, 2H), 4.73−4.82 (m, 3H); ^{13}C NMR ($CDCl_3$, 62.5 MHz) δ 172.1, 166.2, 165.4, 15434, 154.0, 149.0, 145.6, 134.3, 133.9, 133.8, 133.6, 132.7, 129.8, 129.7, 129.4, 129.2, 128.6, 128.4, 85.7, 81.0, 72.7, 70.8, 63.7; IR ($CDCl_3$) ν_{max} 3468, 3384, 3067, 2982, 2874, 1729, 1637, 1602, 1585, 1545, 1452, 1392, 1375, 1316, 1265, 1265, 1178, 1123, 1094, 1070, 786 cm^{-1}; UV−vis (λ_{max}) 231 (53 700 M^{-1} cm^{-1}), 283 (10 960 M^{-1} cm^{-1}), 305 nm (12 300 M^{-1} cm^{-1})

Isolation of 8-Amino-2-methoxy-N⁶,N⁶,O²′,O³′,O⁵′-pentabenzoyladenosine (8). The methanol adduct **8** was obtained as a glassy yellow solid that turned red with time (1.0−1.2 mg, 0.0012−0.0014 mmol, 5−6% yield): $C_{46}H_{36}N_6O_{10}$; molecular weight 832.81 g/mol; mp not available; ^{1}H NMR ($CDCl_3$, 250 MHz) δ 8.32 (d, J = 7.7 Hz, 2H), 7.94 (d, J = 6.9 Hz, 2H), 7.92 (d, J = 6.5 Hz, 2H), 7.81 (d, J = 7.6 Hz, 4H), 7.27−7.59 (complex, 15−16H), 6.39 (d, J = 5.9 Hz, 1H), 6.15 (dd, J = 6.1 Hz, J = 6.1 Hz, 1H), 6.04 (dd, J = 5.4 Hz, J = 5.4 Hz, 1H), 5.80 (bs, 1−2H), 4.70−4.89 (m, 3H) 3.62 (s, 2H); ^{13}C NMR ($CDCl_3$, 62.5 MHz) δ 172.0, 166.2, 165.4, 134.4, 133.8, 133.6, 132.7, 130.0, 129.7, 129.3, 129.1, 128.7, 128.6, 128.5, 128.4, 85.4, 81.1, 72.2, 70.7, 63.8, 55.2, 29.7; IR ($CDCl_3$) ν_{max} 3462, 3381, 3067, 2957, 2928, 2856, 1728, 1639, 1590, 1557, 1480, 1452, 1368, 1316, 1264, 1179, 1125, 1094, 1070, 1026, 820 cm^{-1}; UV−vis (λ_{max}) 230 nm (61 700 M^{-1} cm^{-1}), shoulder at 273 nm (10 500 M^{-1} cm^{-1}), shoulder at 281 nm (9120 M^{-1} cm^{-1}), 326 nm (10 700 M^{-1} cm^{-1}).

Scheme 1

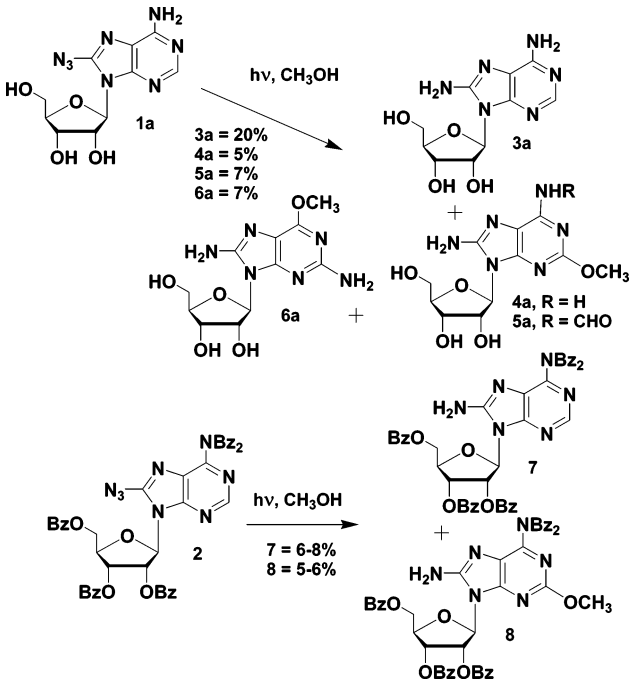

*Oxidation of 8-Aminoadenosine (**3a**) with N-Bromosuccinimide (NBS).* To a stirred solution of 8-aminoadenosine (**3a**) (0.085 g, 0.3 mmol) in CH_3OH (150 mL), at −77 °C, was added a solution of NBS (0.059 g, 0.33 mmol) in CH_3-OH (10 mL). The reaction mixture was allowed to slowly warm to room temperature over the course of 2 h. After 12 h, the reaction was quenched with solid $NaOCH_3$ (1 equiv), and the solvent was removed. The crude mixture was purified by column chromatography (silica gel, 20% CH_3OH in $CHCl_3$) to provide 8-amino-2-methoxyadenosine (**4a**) as a slightly yellow solid (0.062 g, 61%). All spectral data were consistent with an authentic sample obtained as described above.

RESULTS AND DISCUSSION

Chemical Analysis of Photolysis Mixtures. The photolysis (λ > 290 nm) of **1a** has been studied previously in water and found to afford the simple reduction product 8-amino-adenosine (**3a**) as the only identified product (*20*). In the work presented here, the irradiations were conducted using all of the UV lines of an argon ion laser (333.6−363.8 nm) and the reaction products were identified in both methanol and water. Only the products of the methanol reactions have been examined in detail and fully characterized. These are summarized in Scheme 1 along with the products of the benzoylated analogue **2**. The structures of **4a** and **5a** were confirmed by NMR spectroscopy, and the structures of **3a** and **7** were confirmed by comparison with authentic samples. The structure of **6a** was confirmed by X-ray crystallography (Figure 2).

At this point, it is significant to note that the simple 8-amino products, **3a** and **7**, constitute reduction products when referenced to the expected primary photoproduct, the

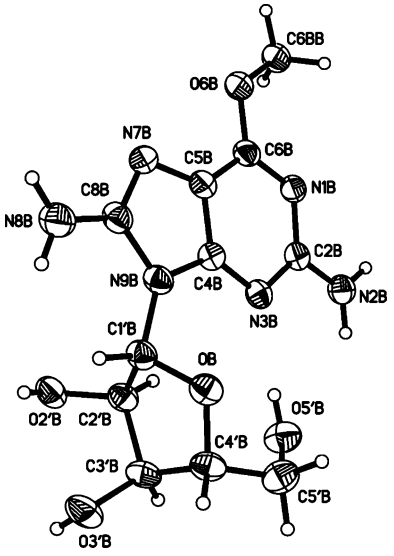

FIGURE 2: X-ray crystal structure of **6a** (only one of the two crystallographically independent molecules is shown).

Scheme 2

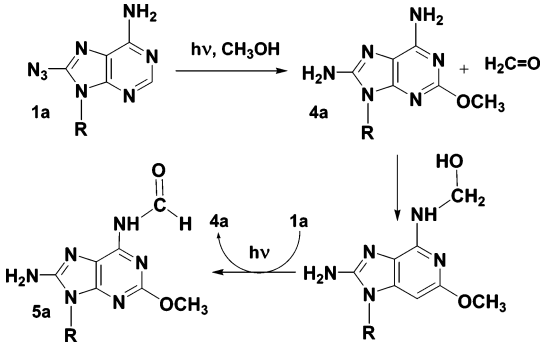

nitrene at the 8-position. All of the other photoproducts are at the same oxidation level as this nitrene. The formation of formamide **5a** is evidence that the solvent methanol is the reducing agent necessary for the formation of **3a** and **7**. A possible mechanism for the formation of **5a** is outlined in Scheme 2. Of course, the ribose moieties might also serve as reducing agents in these reactions, which might help to account for the complexity of the reaction mixtures observed in this chemistry.

Aside from the reduction to the 8-amino compounds, the recurrent theme in these reactions is the addition of the solvent methanol to the purine six-membered ring to form **4a**, **5a**, **6a**, and **8**. Apparently similar adducts can be formed in water and in the presence of secondary amine, but these materials were not characterized because of problems with their purification.

*Photolysis of 8-Azido-N^9-benzyladenine **1b** in Glassy 2MTHF at 77 K.* Cooling of a solution of 8-azido-N^9-benzyladenine **1b** (*22*) in 2-methyltetrahydrofuran (2MTHF) to 77 K leads to the formation of a clear, rigid glass suitable for optical spectroscopy. Upon brief exposure of the glass to 254 nm radiation, the glass turns orange. The orange color does not decay over many hours at 77 K. When the glass is melted, the orange color gradually fades. The UV−vis spectrum of this photoproduct is given as curve 2 of Figure 3, and resembles that of *o*-benzoquinodimethane (*23*). The orange species was generated by irradiation of azide **1b** in a cold 2MTHF glass in the cavity of an EPR spectrometer.

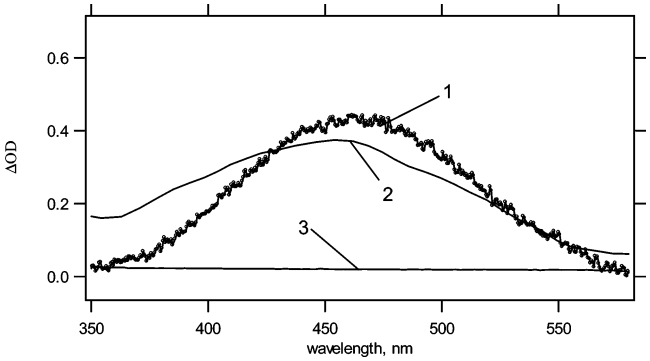

FIGURE 3: Transient absorption spectrum obtained upon irradiation of 8-azidoadenosine **1a** in water (curve 1), persistent spectrum produced by irradiation of **1b** in 2MTHF at 77 K (curve 2), and absorption spectrum of **1a** in water (curve 3).

Scheme 3

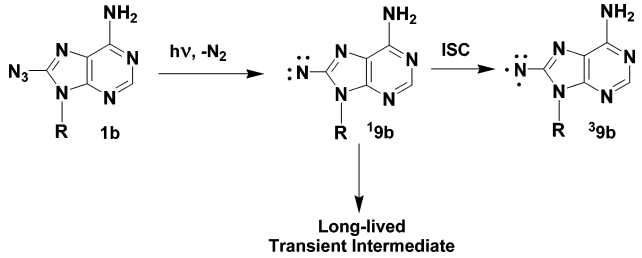

There was no evidence of the presence of a triplet nitrene signal; thus, by EPR spectroscopy, the orange species is not the triplet nitrene ^{3}**9b** (Scheme 3).

*Laser Flash Photolysis (LFP) Studies of 8-Azidoadenosine **1a** and Its Pentabenzoylated Derivative **2**.* Laser flash photolysis (LFP) of 8-azidoadenosine **1a** in water produces the transient spectrum shown as curve 1 of Figure 3. This spectrum is remarkably similar to that produced by photolysis of 8-azido-N^9-benzyladenine **1b** in 2MTHF at 77 K, indicating that related species are observed under both sets of conditions. The species produced by LFP of **1a** shows no decay after 300 μs in water (the maximum observation time of the spectrometer), indicating that its lifetime in water is in excess of 1 ms. In addition, LFP of 8-azidoadenosine **1a** in water produces the same transient absorption in the 400−500 nm range within 400 fs of being irradiated by the exciting laser pulse (the minimum resolvable time of the system) (see the inset in Figure 5). The consistency of these spectroscopic properties over a time ranging from femtoseconds to seconds and even minutes (vide infra) rules out the possibility that this species is a nitrene, in either its singlet

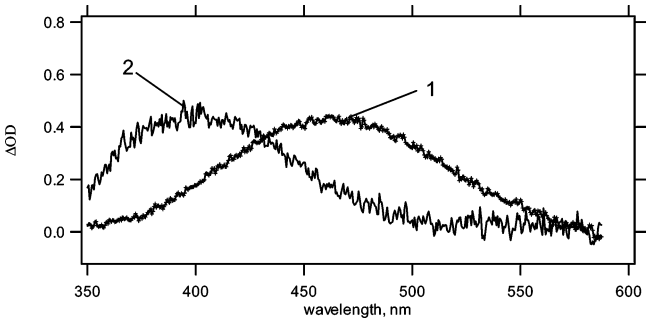

FIGURE 4: Transient absorption spectra produced upon LFP of **1a** in a 50/50 water/acetonitrile mixture (curve 1) and that obtained from LFP of **2** in a 50/50 water/acetonitrile mixture (curve 2).

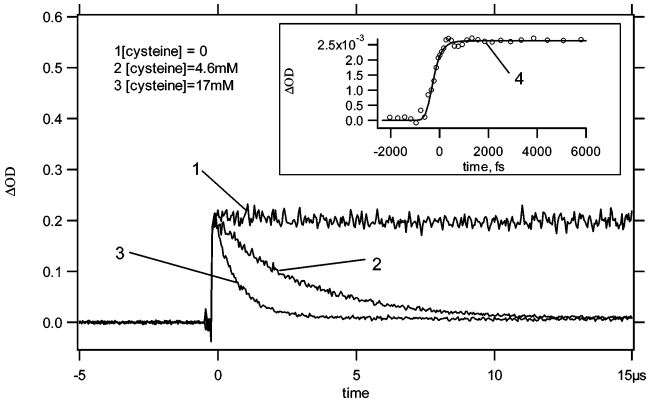

FIGURE 5: Quenching of the 460 nm absorption signal (produced by LFP of **1a**) in HEPES upon addition of increasing concentrations of cysteine (curves 1−3). The inset shows the formation of the 460 nm signal on the femtosecond time scale obtained in a pump and probe experiment (curve 4, fwhm ~ 400 fs).

or triplet state, ^{1}**9a** or ^{3}**9a**, respectively. Furthermore, the rapidity with which this intermediate is formed would seem to indicate that it is derived from the singlet nitrene, if that species has a finite existence at all. Correspondingly, these observations would seem to cast serious doubt on the often-stated view that nitrene **9** is the reactive intermediate present in photoaffinity labeling using 8-azidoadenosine and its analogues.

The known pentabenzoylated derivative of 8-azidoadenosine **2** (*19*) was prepared and its LFP in acetonitrile studied. This compound produced a long-lived species ($\tau \gg 100\ \mu$s) upon LFP with an absorption maximum shifted 50 nm to shorter wavelengths compared to that observed upon LFP of **1a** in water. The transient spectra produced by LFP of **1a** and **2** in a common solvent, 50/50 (v/v) acetonitrile/water mixture, are shown in Figure 4. Since different transient spectra are observed from the two precursors in the same medium, the blue shift of the transient derived from **2** is not a solvent effect, but must be attributed either to a rather significant electronic effect associated with the two benzoyl groups on the 6-amino group or to an intermediate distinctly different from that produced from **1a**. Subsequent data support the latter alternative that **1a** and **2** produce two different types of intermediates, vide infra.

*Quenching of Transient Intermediates Produced by Laser Flash Photolysis (LFP) of 8-Azidoadenosine **1a** and Its Pentabenzoylated Derivative **2**.* The presence of amines, thiols, hydroxide ion, and phenolate ion accelerates the disappearance of the transient absorption spectra shown in Figure 4. Plots of k_{obs}, the pseudo-first-order rate constant of transient decay, versus the concentration of nucleophile are linear (Figures 5 and 6) with slopes equal to the absolute bimolecular rate constants for the reaction of the nucleophile with the transients. The experimentally determined rate constants are given in Table 1.

These data indicate that the reactive intermediates produced both upon photolysis of **1a** in water and **2** in acetonitrile have long lifetimes and high selectivity toward reaction with nucleophiles. At least in the case of **1a**, strong nucleophiles such as alkoxides, phenoxides, thiols, and aliphatic amines are effective trapping agents. However, weaker nucleophiles such as alcohols, phenols, sulfides, and arylamines probably also react with the intermediate, albeit too slowly to be characterized by this LFP method. The

Table 1: Absolute Bimolecular Rate Constants of the Reaction of the Transient Intermediate Produced by LFP of **1a** in the Presence of Nucleophiles at Ambient Temperature

nucleophile	solvent	k (M^{-1} s^{-1})
cysteine	HEPES[a]	6.5×10^7
sodium hydroxide	water	3.6×10^6
diethylamine	water	1.2×10^7
sodium phenoxide	water	*b*
L-tyrosine ethyl ester	HEPES[a]	*c*
L-methionine ethyl ester	HEPES[a]	*c*
L-tryptophan methyl ester	HEPES[a]	*c*
adenosine 5′-monophosphate	HEPES[a]	*c*
uridine	HEPES[a]	*c*
cytidine	HEPES[a]	*c*
guanosine	HEPES[a]	*c*

[a] In 50 mM HEPES and 50 mM KCl at pH 7.6. [b] The reaction kinetics are complex because the product of the reaction also absorbs at 400 nm and is meta-stable. [c] Too slow to measure.

Table 2: Absolute Bimolecular Rate Constants of the Reaction of the Transient Intermediate Produced by LFP of **2** in the Presence of Nucleophiles at Ambient Temperature

nucleophile	k (M^{-1} s^{-1})	nucleophile	k (M^{-1} s^{-1})
diethylamine	3.5×10^7	tetracyanoethylene	*a*
indole	*a*	fumaronitrile	*a*
phenol	*a*	tetrahydrofuran	*a*
pyridine	*a*		

[a] Too slow to measure.

products observed in these reactions (**4a**, **5a**, **6a**, and **8**) certainly confirm that this is the case for methanol.

Furthermore, the rate constants of these reactions demonstrate that the reactive intermediates formed are not so highly reactive that they react indiscriminately with C−H bonds and all nucleophiles in the vicinity of an 8-azidoadenosine-targeted binding site. For the purposes that these photoaffinity labels have been traditionally used, attaching radiolabels to protein molecules and the identification of nucleic acid−protein interactions, this highly selective reactivity may not be desirable. Unless tightly held in a protein binding site, the photogenerated reactive intermediate produced upon photolysis of 8-azidoadenosine and its derivatives may report the presence of potent nucleophiles that are not associated with the natural binding pocket.

Nitrenium Ion Intermediates. The same transient spectrum is observed upon LFP of **2** in acetonitrile (where nitrenium ion formation is not possible) and in CF_3CH_2OH where nitrenium ion formation is most plausible. This argues against assigning the carrier of the aforementioned transient spectra ($\lambda_{max} = 400$ nm; Figure 4) to the corresponding nitrenium ions. Furthermore, the long lifetimes of the transients derived from both **1a** and **2** further argue against assigning these transients to nitrenium ions (*24*, *25*).

Computational Chemistry. While nitrenes and nitrenium ion intermediates have been eliminated as viable intermediates in these reactions, the question remains with regard to the identities of the pivotal 460 and 400 nm absorbing transient intermediates (Figure 4) derived from irradiation of azides **1a** and **2**, respectively. Modern computational methods can be extremely helpful in the determination of various alternatives in cases such as this. For example, CASSCF theory has successfully predicted the energy separation of singlet and triplet phenylnitrenes, their spec-

Scheme 4

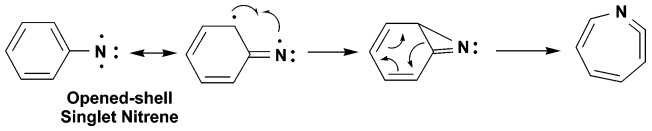

troscopic properties, and the barrier to rearrangement of singlet phenylnitrene into the azepine shown in Scheme 4 (**4** and **5**).

Consequently, the singlet 8-adenylnitrene **^{1}9d** has been studied with CASSCF (8,8) calculations, and the results are summarized in Figure 7. Singlet phenylnitrene (Scheme 4) has an opened-shell, biradical-like, electronic configuration. In contrast, singlet 8-adenylnitrene **^{1}9d** has a closed-shell electronic configuration, because of the presence of zwitterionic resonance structures. The opened-shell singlet configuration of the nitrene is 11 kcal/mol higher in energy than the closed-shell configuration.

As seen in Figure 8, the lowest singlet state of 8-adenylnitrene **^{1}9d** has substantial negative charge on the nitrene nitrogen atom (−0.43) as calculated by a natural population analysis (NPA) (*14*). In contrast, the charge on the same atom in triplet state **^{3}9d** is positive and electron density is shifted into the five-membered ring. The shift in NPA charges upon formation of singlet 8-adenylnitrene **^{1}9d** can be calculated by subtracting the charge on the atom of interest in the parent

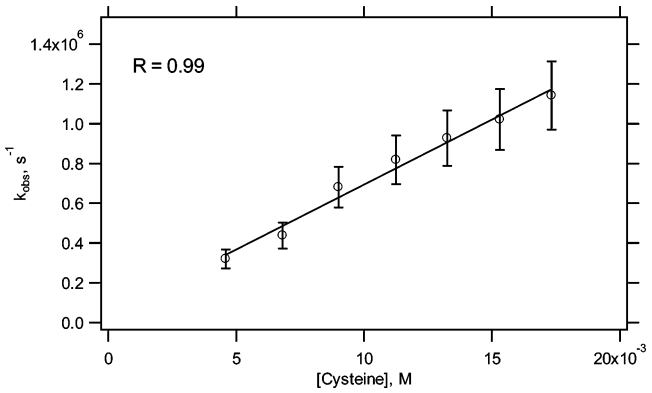

FIGURE 6: Plot of the observed rate constant of the reaction of the species absorbing at 460 nm (produced by LFP of **1a**) with cysteine. The second-order rate constant is 6.5 × 10^7 M^{-1} s^{-1}.

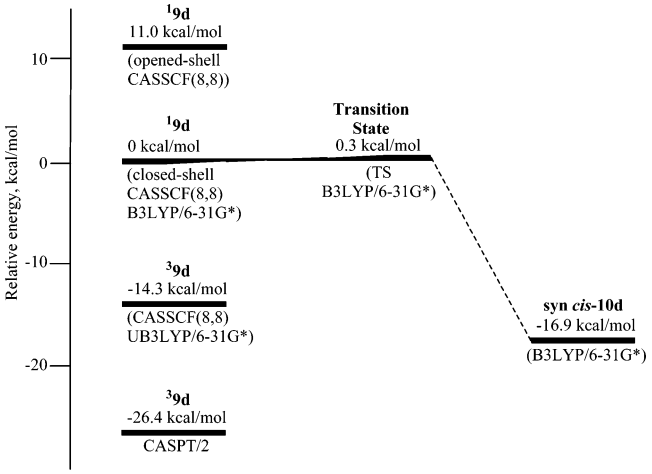

FIGURE 7: Relative energies of nitrene **9d** and opened diazaquinodimethane syn cis-**10d**, obtained by different computational methods.

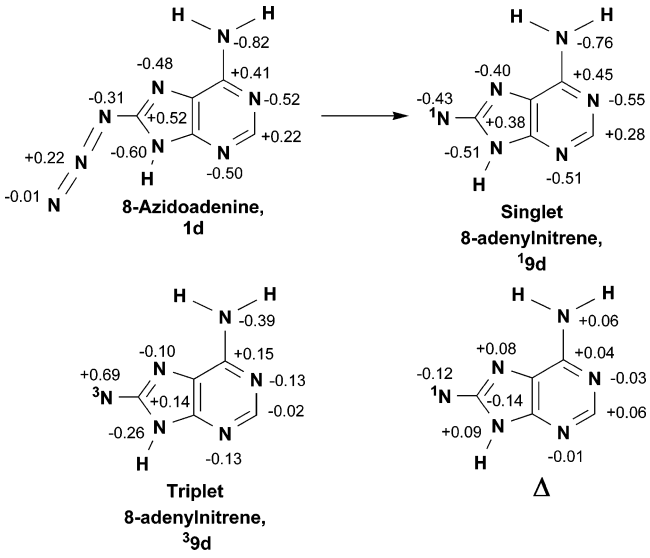

FIGURE 8: Natural population analysis of closed-shell singlet and triplet 8-adenylnitrene (**^{1}9d** and **^{3}9d**), 8-azidoadenine (**1d**), and the shift of charge upon formation of the singlet nitrene (Δ). Calculated using MP2/6-31G*.

Scheme 5

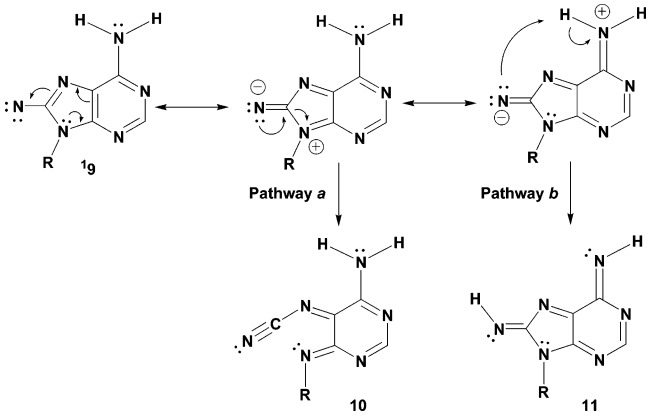

azide molecule **1d** from that of the singlet nitrene **^{1}9d** for the same atom (Δ in Figure 8). According to this analysis, formation of singlet nitrene **^{1}9d** is associated with a shift of negative charge to the nitrene nitrogen and its attached carbon from nitrogens at positions 7 and 9, the 6-amino group, and the six-membered ring in general.

This general charge redistribution is consistent with the selected resonance structures shown in Scheme 5. These resonance structures suggest alternative nitrene reaction pathways that might lead to less reactive intermediates, intermediates that would be expected to be much longer lived then the parent closed-shell singlet nitrene. Pathway *a* would lead to the opened diazaquinodimethane **10** and pathway *b* to the closed diazaquinodimethane **11**.

Fragmentations such as that in pathway *a* are well-documented in heterocyclic azide chemistry as illustrated by the example in Scheme 6 (*25*, *26*). DFT calculations (B3LYP/6-31G*) predict that the barrier to this ring opening is only 0.3 kcal/mol for **^{1}9d** (Figure 7). It is conceivable that this small gas phase barrier may disappear entirely at higher levels of theory or in the condensed phase. In any case, theory predicts that closed-shell singlet nitrene **^{1}9d** will fragment in less than 1 ps to form opened diazaquinodimethane **10**, which is a process that is much faster than that by which

Scheme 6

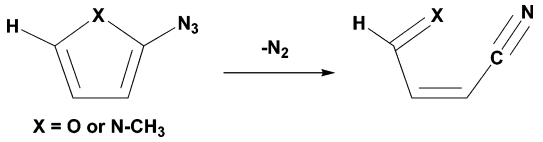

Scheme 7

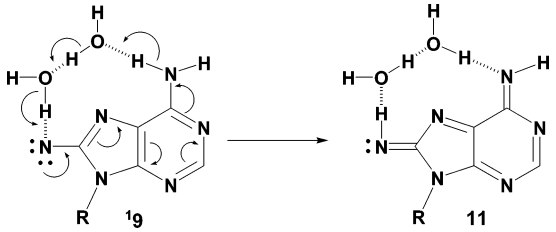

Scheme 8

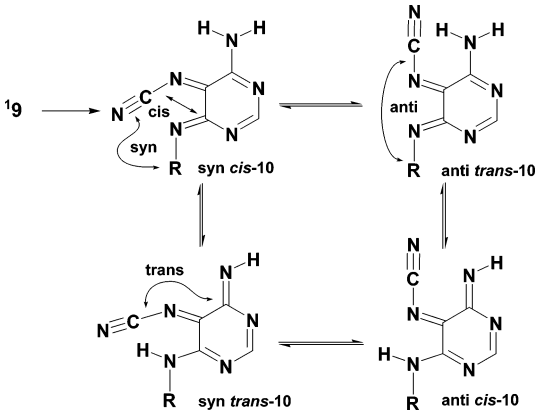

singlet ^{1}**9d** will relax (*5*) to the lower-energy triplet nitrene ^{3}**9d** [which is −14.6 kcal/mol lower in energy by CASSCF (8,8)] or become attached to a biological macromolecular target.

While pathway *b* does not seem to have any parallel in the literature, it might be particularly favorable in the case of adenylnitrene ^{1}**9d**. Thus, the requisite hydrogen or proton shift might occur in a solvent-assisted manner, as shown in Scheme 7, or directly via a tunneling mechanism (*27*) in the absence of a protic environment. Such a tunneling mechanism would be necessary to account for the formation of **11b** in 2MTHF at 77 K. This type of proton shuttle mechanism can proceed on an ultrafast time scale in protic solvents, and may well be competitive with the fragmentation shown in pathway *a*.

In the evaluation of the relative merits of putative intermediates **10** and **11**, at least two additional factors must be taken into consideration. The first of these is that in the case of the opened diazaquinodimethane **10**, arising via pathway *a* in Scheme 5, a family of isomeric tautomers should be in equilibrium with each other as shown in Scheme 8. Thus, the isomer formed initially in fragmentation pathway *a* is syn cis-**10** with the nitrile group syn to the nitrogen bearing the R group and cis with respect to the exocyclic carbon−nitrogen double bond to which it is not directly attached. If ring opening to **10** does occur, then over the long lifetime of the observed intermediate, the initially formed tautomer should have adequate time to become equilibrated with the three other isomeric tautomers of the family.

The second consideration concerns the photochemical behavior of benzoylated adenosine **2**. Benzoylation of the 6-amino group of adenosine will prohibit the proton shuttle mechanism (pathway *b* in Schemes 5 and 7). Consequently, the 400 nm transient observed upon photolysis of **2** cannot be a closed diazaquinodimethane related to **11**. Benzoylation will not affect fragmentation pathway *a* (Scheme 5). However, it will prevent formation of the syn trans and anti cis tautomers related to **10**, and probably significantly inhibit formation of the anti trans tautormer due to the large size of the benzoyl groups (Scheme 8). Therefore, of the possible intermediates suggested in Schemes 5 and 8, only syn cis-**10** would seem to be a viable candidate for the 400 nm transient species observed in the photolysis of **2**.

The situation is by no means as straightforward in parent adenosine system **1a**, where all intermediates outlined in Schemes 5 and 8 would seem to be viable candidates. DFT calculations of the relative energies of **11c** and the family of isomeric tautomers of **10c** shown in Scheme 8 afforded the values shown in Figure 9. These energies were determined in the gas phase using density functional theory (*15*), and in water using the PCM approximation (*13*). It is interesting to note that in aqueous media the initially formed syn cis-**10c** is not the most stable isomeric tautomer, and might be expected to readily isomerize and tautomerize to the most stable anti cis-**10c** tautomer. No indication of this type of equilibrium, which might lead to a shift of the ribose moiety from the 9-position of the adenine ring to the amino group in the 6-position (see Scheme 10), was observed in the products isolated in the photolysis of azidoadenonsine **1a**. Furthermore, and most significantly, these calculations indicated that the closed diazaquinodimethane **11** is the most stable of all intermediates evaluated to date (*28*). At this point, the closed diazaquinodimethane **11a** became the primary candidate for the 460 nm absorbing transient produced in the photolysis of 8-azidoadenosine (**1a**). A complete tabulation of these intermediates along with their calculated relative energies and spectroscopic properties is shown in Figure 10.

TD-DFT (*15*) calculations predict that closed diazaquinodimethane **11c** should exhibit a moderately intense absorption maximum at 430 nm and opened diazaquinodimethane syn cis-**10c** a maximum at 449 nm, both of which are in quite good agreement with the observed value of 460 nm. In contrast, the calculated strong absorption maxima for dibenzoylated analogue **14** are 422 and 411 nm, in excellent agreement with the observed maximum at 400 nm. Thus, benzoylated adenosine **2** clearly affords opened diazaquinodimethane **14**, but the 460 nm transient associated with the parent system, **1a**, might be either the opened or closed diazaquinodimethane related to either **11a** or syn cis-**10a** based upon these data alone. However, DFT calculations also predict that **11c** is 7.8 kcal/mol more stable than syn cis-**10c** in water. Furthermore, the 460 nm transient species formed upon photolysis of **1a** remains unchanged from within 400 fs of photolysis to the millisecond time domain. If this intermediate were an opened diazaquinodimethane, then the equilibrium outlined in Scheme 8 should be active and cause a shift in the transient absorption from ca. 449 to 474 nm. No such time-dependent red shift was observed. In addition, the DFT calculations indicate that within the family of tautomeric isomers in Scheme 8, anti cis-**10** is the most

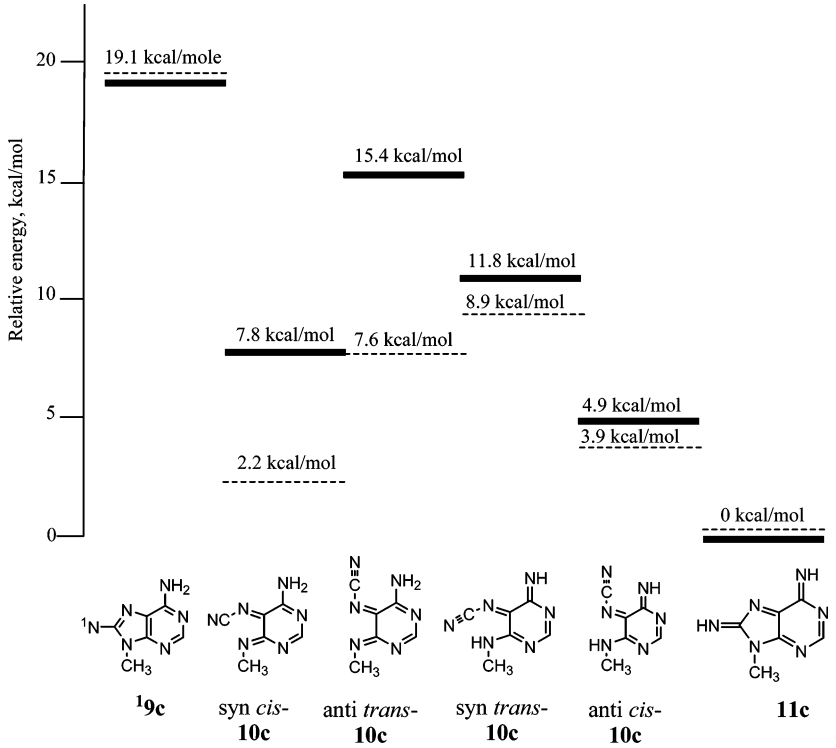

FIGURE 9: Relative energy diagram obtained by B3LYP(6-31G*) calculations for different intermediates in the gas phase (dashed line) and in water using the PCM solvent model (solid line).

Scheme 9

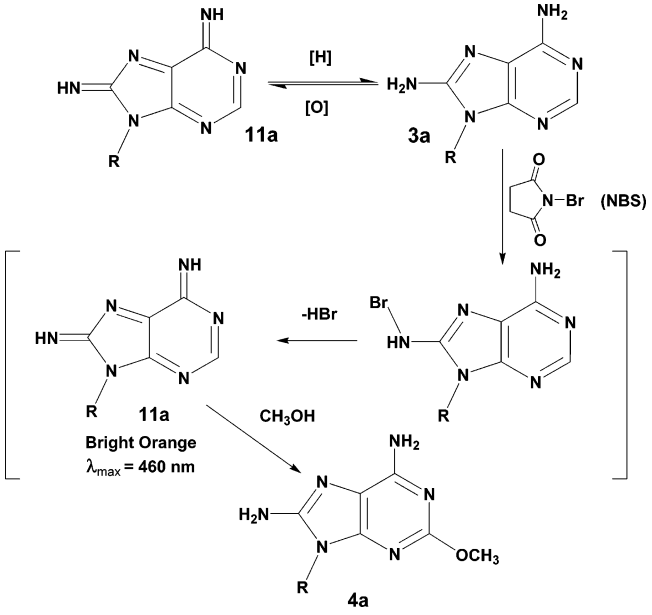

Scheme 10

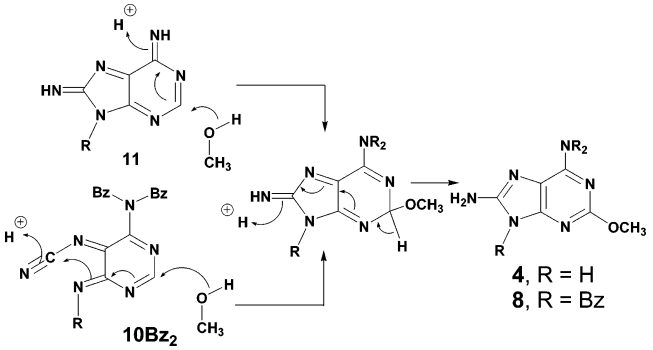

stable, and were this form to undergo nucleophilic addition (see Scheme 10), the product would have the ribose attached to the 6-amino group instead of its usual site of attachment at the 9-position. No such products were observed. Finally, the assignment of the 460 nm transient to the closed diazaquinodimethane **11a** is also consistent with the formation of the same intermediate via the NBS oxidation of 8-aminoadenosine discussed in a later section (see Scheme 9).

DFT calculations predict that syn cis-**10c** will have a C═N ring vibration at 1229 cm^{-1} [after applying a scaling coefficient 0.98 (*29*)]. LFP of benzoylated analogue **2** in acetonitrile with IR detection gives the transient spectrum of Figure 11 in which a peak at 1229 cm^{-1} is detected. The carrier of the 1229 cm^{-1} band reacts with diethylamine with approximately the same absolute rate constant as does the carrier of the 400 nm transient absorption ($k = 3.5 \times 10^7$ M^{-1} s^{-1}) within experimental error. This is further evidence that the nitrene produced by photolysis of **2** cleaves to the benzoylated opened diazaquinodimethane analogue of syn cis-**10**. Unfortunately, TRIR experiments are not feasible in water because of the broad IR absorbance of this solvent. We could not study the photochemistry of **1a** in acetonitrile because of its poor solubility in this solvent.

On the basis of the aforementioned evidence, it is clear that while a nitrene species is probably involved in the photochemistry of 8-azidoadenosine (**1a**) and its derivatives, it very rapidly (femtoseconds) undergoes a hydrogen relocation to form closed diazaquinodimethane **11a**. In the absence of nucleophiles, this species has a lifetime of seconds to minutes and is the pivotal reactive species involved in photoaffinity labeling. If the pathway to **11** is blocked, as in the case of **2**, the corresponding nitrene can rapidly undergo fragmentation of the five-membered ring to form opened

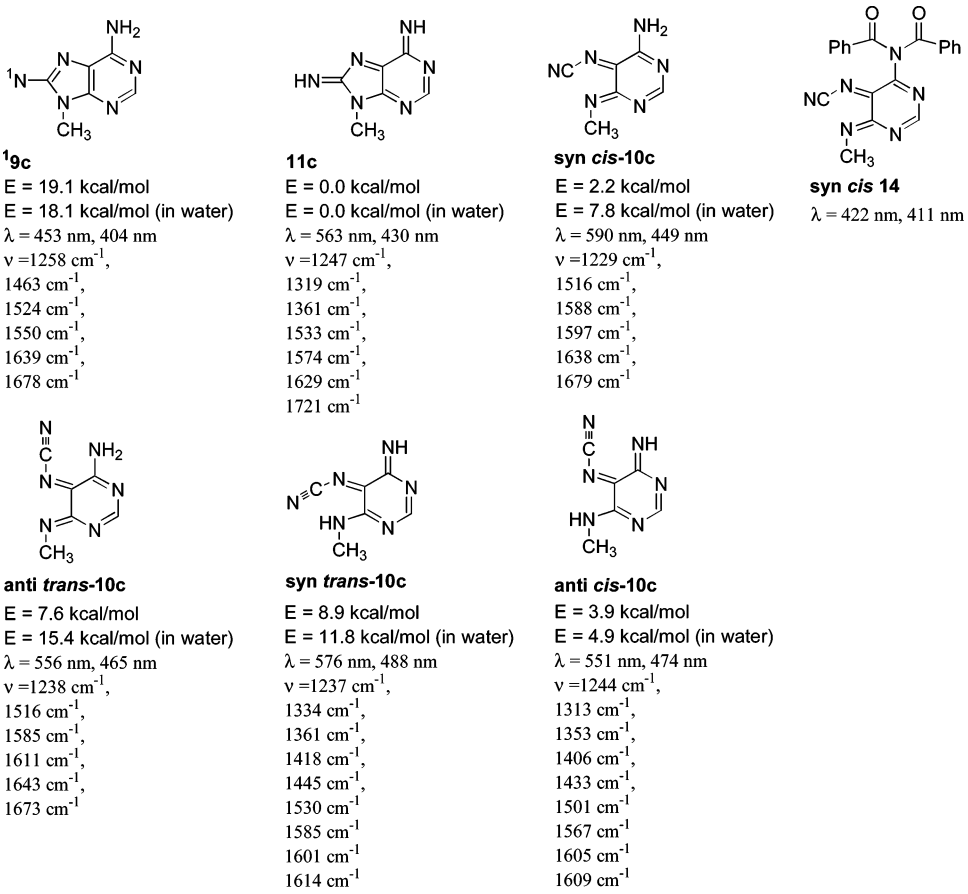

FIGURE 10: Relative energies of **11** and the tautomers of **10** in water as determined by DFT, their principle vibrations, and gas phase electronic transitions predicted by TD-DFT.

FIGURE 11: Transient absorption IR spectrum obtained upon LFP of the pentabenzoylated 8-azidoadenosine **2** in acetonitrile.

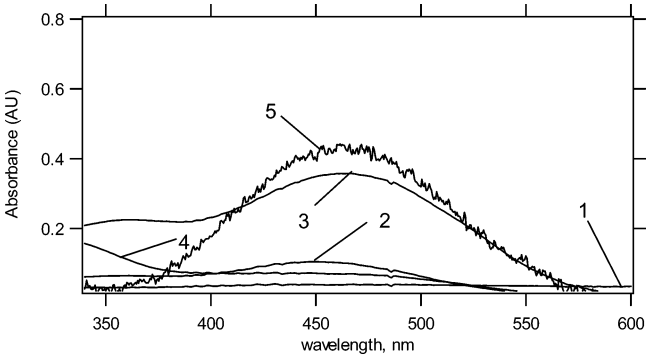

FIGURE 12: Persistent UV spectrum of **11a** produced by NBS oxidation of **1a** in methanol at −75 °C. Curve 1 is the spectrum of the starting material, curve 2 when a small amount of NBS was added, curve 3 after further addition of NBS, curve 4 upon completion of the reaction at ambient temperature, and curve 5 the absorption spectrum produced upon LFP of **1a** in a 50/50 water/acetonitrile mixture (10 ns after the pulse).

diazaquinodimethane **10**, which seems to have chemistry quite similar to that of **11**.

*Chemistry of Diazaquinodimethanes **10** and **11**.* As their names imply, the opened and closed diazaquinodimethanes **10** and **11** would be expected to have quinone-like chemistry. If this is true, then they should undergo rather facile oxidation−reduction chemistry. This correlation is shown in Scheme 9 for **11a**. Thus, it is probably the simple reduction of **11a**, and not of nitrene ^{1}**9a**, that accounts for the formation of **3a** in the reactions shown in Scheme 9, and the formation of **7** from the corresponding opened diazaquinodimethane related to **10**. This correlation is supported by the observation of formate **5a** (Scheme 2). Furthermore, we reasoned that if this oxidation−reduction chemistry is facile, then it should be possible to oxidize 8-aminoadenosine (**3a**) to the same intermediate that was observed in the azide photolysis and observe its trapping with methanol. A number of oxidizing agents and conditions were examined with this end in mind. The best of these was found to be NBS in methanol as a solvent at −75 °C. Thus, when **3a** is dissolved in methanol, the solution cooled to −75 °C, and a solution of NBS added, the reaction mixture immediately becomes bright orange with the UV−vis spectrum shown as curve 3 in Figure 12. This spectrum agrees well with the spectrum produced upon LFP of **1a** in water. It was most interesting to observe that when the solution is warmed to ambient temperature, the orange intermediate persisted for minutes before the solution faded

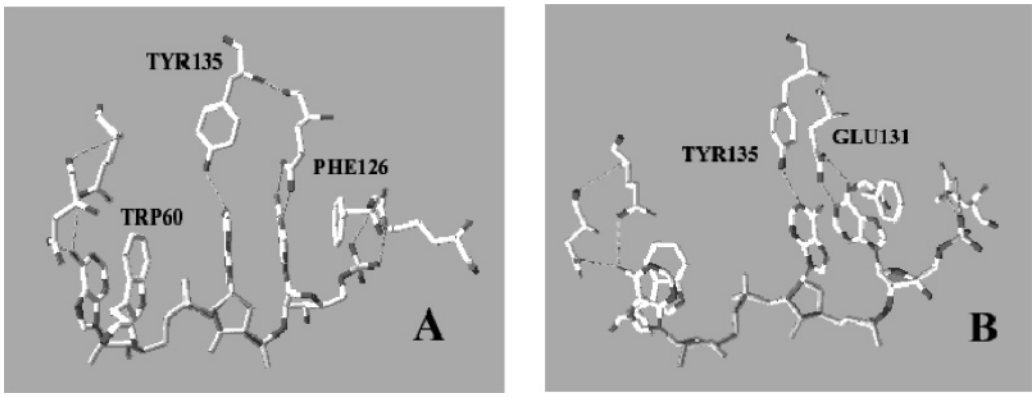

FIGURE 13: Active site for the binding of 5′-phosphate of 2′,5′-triadenylate to human ribonuclease L. Panel A emphasizes the π-stacking interactions between Trp60 and the 2′-terminal adenylate and the remaining two adenylates and Phe126. Panel B emphasizes the hydrogen bonding interaction at the Watson−Crick edge between the 5′-terminal adenylate and Glu131 and between the central adenylate and Tyr135.

to pale yellow as shown in Figure 12. Furthermore, only a single product was formed in this NBS reaction, and upon isolation and characterization, this product proved to be methanol adduct **4a**. No trace of isomeric methanol adduct **6a** could be found in this reaction. This NBS oxidation experiment provides further strong evidence that the reactive intermediate produced upon LFP of **1a** is closed species **11a** (corresponding to pathway *b* of Scheme 5) as we think it is unlikely that 8-aminoadenosine will both oxidize and ring open to the higher-energy tautomer syn cis-**10a** under these conditions.

On the basis of these observations, it seems reasonable to assign the pivotal trapping reaction of 8-azidoadenosine photoaffinity labeling to a Michael addition or 1,4-addition of nucleophiles to closed diazaquinodimethane **11a** as outlined in Scheme 10. A closely related Michael addition should also be active in open diazaquinodimethane **10Bz$_2$** derived from benzoylated analogue **2**, which also is outlined in Scheme 10.

Finally, it is interesting to note that this work explains why previous investigators (*30*−*32*) have identified tyrosine residues as the sites of covalent attachment of the intermediate produced upon photolysis of **1a** and its analogues. Particularly interesting is the observation of Wower et al. (*33*), who obtained the same labeling of bovine ribonuclease A upon irradiation of a solution of the protein and 8-azidoadenosine **1a** together, and when the azide was irradiated alone in buffer, followed by the addition of the previously photolyzed solution of **1a** to the protein in the dark. The very long lifetime of reactive diazaquinodimethane **11a** is completely consistent with these observations.

One question remains. What is the mechanism of formation of rearranged methanol adduct **6a**? This isomer constitutes the result of a trapping mechanism that is apparently significantly different from that leading to **4a**. Adducts of type **6** may be particularly significant, since if water were the trapping agent, which preliminary studies indicate occurs in a manner comparable to trapping with methanol, 8-aminoguanosine would be the expected trapping product. That is, insofar as the Watson−Crick binding edge of the nucleotide is concerned, an adenosine edge could be photochemically transformed into a guanosine edge. For these reasons, we have explored a number of possible mechanisms for the formation of **6**. A priori, one might conceive of a photoisomerization of **4** to **6**. However, irradiation of **4a** does not afford any detectable quantities of **6a**. Singlet oxygen might conceivably give rise to **6a** from **3a**. However, irradiation of **3a** in a methanolic solution of rose bengal using visible light does not afford **6a**. The only firm correlation that we have been able to establish at this time is that the formation of **6a** from **1a** is oxygen-dependent. Thus, irradiation of a degassed solution of **1a** affords only **4a** and no **6a**. In contrast, irradiation of **1a** under aerobic conditions or under an oxygen atmosphere affords the usual amount of **6a** reported earlier in this paper. Since singlet nitrene ^{1}**9a**, **4a**, and **6a** are all at the same oxidation level, the role of oxygen in the formation of **6a** cannot be that of an oxidizing agent. Consequently, oxygen is most likely serving simply as a spin trap in a radical reaction the exact nature of which is unknown at this time.

*Implications of Photoaffinity Labeling with 8-Azidoadenosine (**1a**) and Its Derivatives.* It is conspicuously clear from this study that photolysis of 8-azidoadenosine (**1a**) and its derivatives does not produce a highly reactive species that reacts indiscriminately with proteins and nucleic acids in its immediate vicinity at a rate approaching diffusion controlled. Instead, such photolyses produce the reactive, but selective, closed diazaquinodimethane **11** that reacts fairly rapidly with amines and thiols, but only relatively slowly with weak neutral oxygen nucleophiles such as alcohols and phenols. This means that caution needs to be exercised to be sure that the binding site is indeed effectively targeted. If diazaquinodimethane **11** does not react effectively at the original binding site, but wanders and becomes attached to a remote site, false binding site information will be obtained. This is not a serious problem in studies where the goal is simply to label or cross-link protein targets. However, it might become a significant issue in studies aimed at obtaining specific binding site information. In cases such as these, transient spectroscopic studies will become a requisite component of any photoaffinity labeling study.

As the photoaffinity labeling technique becomes increasingly refined and extended to more complex systems involving oligonucleotides, the binding problems should become less of a concern, since the labeling compound will be held in place by multiple binding interactions. An excellent example of how this might work can be seen in the interaction of the 5′-phosphate of 2′,5′-linked triadenylate with the N-terminal repeat domain of human RNase L (*34*). As shown in Figure 13, the triadenylate is bound by many

hydrogen bonding and π-stacking interactions. Thus, a long-lived transient will likely remain attached to the original binding site long enough to react with one of the interacting amino acid residues.

It is also worth noting that generation of an extremely electron deficient diazaquinodimethane at any of the sites involved in π-stacking interactions (Figure 13A) should lead to stronger bonding than in the parent azide. Also, this same π-stacking interaction might well affect the 460 nm absorption band of diazaquinodimethane **11** and provide useful information about the environment of this species over its lifetime. Consequently, extension of the transient studies begun in this work into protein environments would be highly desirable and most interesting.

Finally, previous a priori mechanisms for photoaffinity labeling with 8-azidoadenosine all invoked attachment of the nitrene nitrogen to the protein framework. Upon reflection, this is not correct, since in the typical anti conformation of nucleotides, the 8-position of the adenine is on a Hoogsteen edge. The substituent on the 8-position is not usually involved in noncovalent binding to the target molecule, and is generally less accessible than atoms along the Watson−Crick edge. As has been shown in this study, the adenine sites that become active upon photolysis of 8-azidoadenosine and its derivatives and susceptible to nucleophilic attack reside along the Watson−Crick edge. Since this is the edge that is usually involved in binding to the target sites, and since this binding frequently involves groups that can serve as nucleophiles, 8-azidoadenosine is in some respects a well-engineered photoaffinity labeling reagent. Tyrosine residues seem to be particularly effective traps of diazaquinodimethane related to **11a**. While tyrosine, tryptophan, and phenylalanine are frequently involved in π-stacking interactions, which might make them good trapping targets, in the example shown in Figure 13B, tyrosine residues also can be involved in a hydrogen bonding interaction along the Watson−Crick edge. This makes tyrosine residues ideal trapping targets, as has been observed by previous workers (*30*−*32*).

CONCLUSIONS

Photolysis of 8-azidoadenosine (**1a**) in water or buffer releases a singlet nitrene, which has a lifetime of less than 400 fs. The singlet nitrene undergoes a hydrogen shift to form a closed azaquinodimethane (**11a**) faster then it can relax to a triplet nitrene or react with a biological target molecule. This species has a lifetime of several minutes in the absence of good nucleophiles, and is the species which forms adducts in cross-linking and photoaffinity labeling experiments via selective reactions with nucleophiles such as amines, thiols, and phenolate ions. Because of the selective reactivity of this closed diazaquinodimethane **11a**, one must recognize that it may wander from its original binding site and become attached to a nucleophilic residue at a remote site. The observations reported here suggest that conclusions derived from cross-linking experiments using 8-azidoadenosine and its derivatives should be viewed with caution. On the other hand, the mechanistic picture afforded by this work should be of significant value in planning photoaffinity labeling strategies and the interpretation of future results obtained from photoaffinity labeling experiments with the family of 8-azidoadenosine reagents.

ACKNOWLEDGMENT

R.M.W. thanks Professor Neocles Leontis of Bowling Green State University (Bowling Green, OH) for most helpful discussions of RNA binding motifs. The authors thank the OSU Center for Chemical and Biophysical Dynamics for the use of their facilities.

SUPPORTING INFORMATION AVAILABLE

Figures depicting ultrafast kinetics and spectra recorded on pico- and nanosecond time scales along with the Cartesian coordinates of the optimized geometries of the reactive intermediates. This material is available free of charge via the Internet at http://pubs.acs.org.

REFERENCES

1. Haley, B. E. (1983) Development and Utilization of 8-Azidopurine Nucleotide Photoaffinity Probes, *Fed. Proc. 42*, 2831−2836.
2. (a) Meisenheimer, K. M., and Koch, T. H. (1997) Photocross-linking of Nucleic Acids to Associated Proteins, *Crit. Rev. Biochem. Mol. Biol. 32*, 101−140. (b) Cartwright, I. L., and Hutchinson, D. W. (1980) Azidopolynucleotides as Photoaffinity Reagents, *Nucleic Acids Res. 8*, 1675−1691. (c) Fleming, S. A. (1995) Chemical reagents in Photoaffinity Labeling, *Tetrahedron 51*, 12479−12520. (d) Bayley, H. (1983) *Photogenerated Reagents in Biochemistry and Molecular Biology*, Vol. 12, Elsevier, New York. (e) Hatanaka, Y., Nakayama, H., and Kanaoka, Y. (1996) Diazirine-Based Photoaffinity Labeling: Chemical Approach to Biological Interfaces, *Rev. Heteroat. Chem. 14*, 213−243.
3. (a) Sylvers, L. A., and Wower, J. (1993) Nucleic Acid-Incorporated Azidonucleotides: Probes for Studying the Interaction of RNA or DNA with Proteins and Other Nucleic Acids, *Bioconjugate Chem. 4*, 411−418. (b) Hanna, M. M., Bentsen, L., Lucido, M., and Sapre, A. (1999) RNA-Protein Cross-linking with Photoreactive Nucleotide Analog, *Methods Mol. Biol. 118*, 21−33. (c) Hanna, M. M. (1989) Photoaffinity Cross-linking methods for studying RNA-Protein Interaction, *Methods Enzymol. 180*, 383−409.
4. Karney, W. L., and Borden, W. T. (1997) Ab Initio Study of the Ring Expansion of Phenylnitrene and Comparison with the Ring Expansion of Phenylcarbene, *J. Am. Chem. Soc. 119*, 1378−1387.
5. Gritsan, N. P., Zhu, Z., Hadad, C. M., and Platz, M. S. (1999) Laser Flash Photolysis and Computational Study of Singlet Phenylnitrene, *J. Am. Chem. Soc. 121*, 1202−1207.
6. Martin, C. B., Shi, X., Tsao, M.-L., Karweik, D., Brooke, J., Hadad, C. M., and Platz, M. S. (2002) The Photochemistry of Riboflavin Tetraacetate and Nucleosides. A Study Using Density Functional Theory, Laser Flash Photolysis, Fluorescence, UV−Vis, and Time-Resolved Infrared Spectroscopy, *J. Phys. Chem. B 106*, 10263−10271.
7. Martin, C. B., Tsao, M.-L., Hadad, C. M., and Platz, M. S. (2002) The Reaction of Triplet Flavin with Indole. A Study of the Cascade of Reactive Intermediates Using Density Functional Theory and Time-Resolved Infrared Spectroscopy, *J. Am. Chem. Soc. 124*, 7226−7234.
8. (a) Roos, B. O. (1987) The complete active space self-consistent field method and its applications in electronic structure calculations, *Adv. Chem. Phys. 69*, 399−445. (b) Roos, B. O. (1980) The complete active space SCF method in a Fock-Matrix-based super-CI formulation, *Int. J. Quantum Chem., Symp. 14*, 175−189.
9. Hariharan, P. C., and Pople, J. A. (1973) Influence of polarization functions on MO hydrogenation energies, *Theor. Chim. Acta 28*, 213−222.
10. (a) Anderson, K., Malmqvist, P.-Å., and Roos, B. O. (1992) Second-order perturbation theory with a complete active space self-consistent field reference function, *J. Chem. Phys. 96*, 1218−1226. (b) Anderson, K., and Roos, B. O. (1993) Multiconfigurational second-order perturbation theory: A test of geometries and binding energies, *Int. J. Quantum Chem. 45*, 591−607.
11. Andersson, K., Barysz, M., Bernhardsson, A., Blomberg, M. R. A., Cooper, D. L., Fleig, T., Fülscher, M. P., de Graaf, C., Hess, B. A., Karlström, G., Lindh, R., Malmqvist, P.-Å., Neogrády, P., Olsen, J., Roos, B. O., Sadlej, A. J., Schütz, M., Schimmelpfennig,

B., Seijo, L., Serrano-Andrés, L., Siegbahn, P. E. M., Stålring, J., Thorsteinsson, T., Veryazov, V., and Widmark, P.-O. (2000) *MOLCAS*, version 5, Lund University, Lund, Sweden.

12. (a) Becke, A. D. (1993) Density-functional thermochemistry. III. The role of exact exchange, *J. Chem. Phys. 98*, 5648−5652. (b) Lee, C., Yang, W., and Parr, R. G. (1988) Development of the Colle-Salvetti correlation-energy formula into a functional of the electron density, *Phys. Rev. B 37*, 785−789. (c) Miehlich, B., Savin, A., Stoll, H., and Preuss, H. (1989) Results obtained with the correlation energy density functionals of Becke and Lee, Yang and Parr, *Chem. Phys. Letters 157*, 200−206.
13. (a) Miertus, S., Scrocco, E., and Tomasi, J. (1981) Electrostatic interaction of a solute with a continuum. A direct utilization of ab initio molecular potentials for the prevision of solvent effects, *Chem. Phys. 55*, 117−129. (b) Miertus, S., and Tomasi, J. (1982) Approximate evaluations of the electrostatic free energy and internal energy changes in solution processes, *Chem. Phys. 65*, 239−245. (c) Barone, V., Cossi, M., and Tomasi, J. (1997) A new definition of cavities for the computation of solvation free energies by the polarizable continuum model, *J. Chem. Phys. 107*, 3210−3221. (d) Barone, V., Cossi, M., and Tomasi, J. (1998) Geometry optimization of molecular structures in solution by the polarizable continuum model, *J. Comput. Chem. 19*, 404−417.
14. Reed, A. E., Weinhold, F., Curtiss, L. A., and Pochatko, D. J. (1986) Natural bond orbital analysis of molecular interactions: Theoretical studies of binary complexes of hydrogen fluoride, water, ammonia, molecular nitrogen, molecular oxygen, carbon monoxide, and carbon dioxide with hydrogen fluoride, water, and ammonia, *J. Chem. Phys. 84*, 5687−5705.
15. Casida, M. E., Jamorski, C., Casida, K. C., and Salahub, D. R. (1998) Molecular excitation energies to high-lying bound states from time-dependent density-functional response theory: Characterization and correction of the time-dependent local density approximation ionization threshold, *J. Chem. Phys. 108*, 4439−4449.
16. Frisch, M. J., Trucks, G. W., Schlegel, H. B., Scuseria, G. E., Robb, M. A., Cheeseman, J. R., Zakrzewski, V. G., Montgomery, J. A., Jr., Stratmann, R. E., Burant, J. C., Dapprich, S., Millam, J. M., Daniels, A. D., Kudin, K. N., Strain, M. C., Farkas, O., Tomasi, J., Barone, V., Cossi, M., Cammi, R., Mennucci, B., Pomelli, C., Adamo, C., Clifford, S., Ochterski, J., Petersson, G. A., Ayala, P. Y., Cui, Q., Morokuma, K., Salvador, P., Dannenberg, J. J., Malick, D. K., Rabuck, A. D., Raghavachari, K. Foresman, J. B., Cioslowski, J., Ortiz, J. V., Baboul, A. G., Stefanov, B. B., Liu, G., Liashenko, A., Piskorz, P., Komaromi, I., Gomperts, R., Martin, R. L., Fox, D. J., Keith, T., Al-Laham, M. A., Peng, C. Y., Nanayakkara, A., Challacombe, M., Gill, P. M. W., Johnson, B., Chen, W., Wong, M. W., Andres, J. L., Gonzalez, C., Head-Gordon, M., Replogle, E. S., and Pople, J. A. (2001) *GAUSSIAN 98*, revision A.11.1, Gaussian, Inc., Pittsburgh, PA.
17. Houštěk, J., and Smrt, J. (1979) Synthesis of 8-Azidoadenosine 5′-Phosphate, *Collect. Czech. Chem. Commun. 44*, 976−980.
18. Holmes, R. E., and Robins, R. K. (1965) Purine nucleosides. IX. The synthesis of 9-β-D-ribofuranosyluric acid and other related 8-substituted purine ribonucleosides, *J. Am. Chem. Soc. 87* (8), 1772−1776.
19. Charubala, R., Pfleiderer, W., Sobol, R. W., Li, S. W., and Suhadolnik, R. J. (1989) Nucleotides. Part XXX. Chemical synthesis of adenylyl-(2′→5′)-adenylyl-(2′→5′)-8-azidoadenosine, and activation and photoaffinity labeling of RNase L by [^{32}P]-p5′A2′p5′A2′p5N38A, *Helv. Chim. Acta 72*, 1354−1361.
20. Bose, S. N. (1984) Photolysis of 8-azidoadenosine, *Indian J. Chem. 23B*, 677.
21. *SMART*, version 5.631, and *SAINT*, version 6.45A (2004) Bruker Analytical X-ray Instruments, Inc., Madison, WI. Sheldrick, G. M. (2004) *SADABS*, version 2.10, University of Göttingen, Göttingen, Germany. Sheldrick, G. M. *SHELXTL*, version 6.14, University of Göttingen, Göttingen, Germany, and Bruker Analytical X-ray Instruments, Inc., Madison, WI.
22. 9-Benzyladenine [Kikugawa, Y. S. (1981) A Facile N-Alkylation of Imidazides and Benzimidazides, *Synthesis 2*, 124−125] was brominated to form the 8-bromo derivative and then treated with sodium azide to form 8-azido-9-benzyladenine as described for the parent system.
23. Tseng, K. L., and Michl, J. (1977) An approach to biradical-like species. Spectroscopy of *o*-xylylene in argon matrix, *J. Am. Chem. Soc. 99*, 4840−4842.
24. Srivastava, S., Ruane, P., Toscano, J. P., Sullivan, M. B., Cramer, C. J., Chiapperino, D., Reed, E. C., and Falvey, D. E. (2000) Structures of Reactive Nitrenium Ions: Time-Resolved Infrared Laser Flash Photolysis and Computational Studies of Substituted *N*-Methyl-*N*-arylnitrenium Ions, *J. Am. Chem. Soc. 122*, 8271−8278.
25. Gadosy, T. A., and McClelland, R. A. (1999) Photochemistry of 2-azido-1-methylimidazole in aqueous solutions. Observation of the 1-methyl-2-imidazolylnitrenium ion, *J. Am. Chem. Soc. 121*, 1459−1465. Since these workers had observed protonation of an imidazole nitrene to a nitrenium ion, we used DFT methods to examine this process for **^{1}9d** reacting with HCl. We found this process predicted to be 110 kcal/mol exothermic in water, and the resulting nitrenium ion to have a predicted UV−vis absorption maximum at 502 nm [TD-DFT calculations (*15*)]. This line of research was not pursued further, since the transient(s) generated from a nitrenium ion precursor did not seem to be related to those generated from the 8-azido systems, and since additional calculations indicated that the nitrenium ion was a global minimum that was not prone to forming the intermediates related to the 8-azido systems.
26. (a) Dehaen, W., and Becher, J. (1993) Ring-Opening of Five-Membered Heteroaromatic Azides and Nitrenes, *Acta Chem. Scand. 47*, 244−254. (b) Funicello, M., Spagnolo, P., and Zanirato, P. (1993) Intramolecular Cyclizations and Ring-Cleavage Reactions of Five-Membered Hetero-arylnitrenes and their Precursors, *Acta Chem. Scand. 47*, 231−243. (c) Spinelli, D., and Zanirato, P. (1993) On the Chemical, NMR and Kinetic Properties of 2-Azido- and 3-Azidothiophene: Recent Developments, *J. Chem. Soc., Perkin Trans. 2*, 1129−1133.
27. For a general review of quantum mechanical tunneling, see: Bell, R. P. (1980) *The Tunnel Effect in Chemistry*, Chapman and Hall, London. In this example, the proton transfer is likely a two-step process in which a hydrogen migrates first from the amino group attached to C6 to N7 and then from N7 to the nitrogen atom attached to C8.
28. Other possible structures were evaluated by these methods, but were found to be much higher in energy and were not considered further.
29. Scott, A. P., and Radom, L. (1996) Harmonic Vibrational Frequencies: An Evaluation of Hartree−Fock, Møller−Plesset, Quadratic Configuration Interaction, Density Functional Theory, and Semiempirical Scale Factors, *J. Phys. Chem. 100*, 16502−16513.
30. (a) Bubis, J., and Taylor, S. S. (1985) Covalent Modification of both cAMP Binding Sites in cAMP Dependent Protein Kinase I by 8-Azidoadenosine 3′,5′-Monophosphate, *Biochemistry 24*, 2163−2170. (b) Kerlavage, A. R., and Taylor, S. S. (1980) Covalent Modification of an Adenosine 3′:5′-Monophosphate Binding Site of the Regulartory Subunit of cAMP-dependent Protein Kinase II with 8-Azidoadenosine 3′:5′-Monophosphate, *J. Biol. Chem. 255*, 8483−8488.
31. Koh, D. W., Patel, C. N., Ramsinghani, S., Slama, J. T., Oliveira, M. A., and Jacobson, M. K. (2003) Identification of an Inhibitor Binding Site of Poly (ADP-ribose) Glycohydrolase, *Biochemistry 42*, 4855−4863.
32. Rush, J., and Konigsberg, W. H. (1990) Photoaffinity Labeling of the Klenow Fragment with 8-azido-dATP, *J. Biol. Chem. 265*, 4821−4827.
33. Wower, J., Aymie, M., Hixson, S. S., and Zimmerman, R. A. (1989) Photochemical Labeling of Bovine Ribonuclease A with 8-Azidoadenosine 3′,5′-Biphosphate, *Biochemistry 28*, 1563−1567.
34. Tanaka, N., Nakanishi, M., Kusakabe, Y., Goto, Y., Kitade, Y., and Nakamura, K. T. (2004) Structural Basis for Recognition of 2′,5′-Linked Oligoadenylates by Human Ribonuclease L, *EMBO J. 23*, 3939−3938.

BI050859Z